News from viscousland

Corinne Vachier[1] and Fernand Meyer[2]

[1] *Centre de mathématiques et de leurs applications (CMLA), Ecole Normale Supérieure de Cachan, France*
Corinne.Vachier@cmla.ens-cachan.fr

[2] *Centre de Morphologie Mathématique (CMM), Ecole des Mines de Paris, Fontainebleau, France*
Fernand.Meyer@cmm.ensmp.fr

Abstract Viscous closings have been presented at ISMM'02 as an efficient tool for regularizing the watershed lines in gray-scale images. We consider now the problem of reconnecting several edge portions of a same object. In the binary case, this is very nicely solved via the computation of the distance function to the grains: the downstream of the saddle points reconnects the grains, and is known as the perceptual graph. As a particular case, overlapping particles may be separated by computing the watershed line of the inverse distance function. This paper extends the approach to grey-tone images using the concept of viscous dilations. Finally, combinations of both viscous dilations and viscous closings are proposed for segmenting objects with dotted and irregular contours.

Keywords: morphological filtering, viscous closing, viscous dilation, crest line.

1. Introduction

Crest lines of numerical functions play a fundamental role in many image analysis applications. In segmentation for example crest lines of gradient images coincide with shapes edges. And there are many other situations where crest lines are meaningful: road detection in air images, vessel extraction in medical images or writing analysis... (see Figure 1).

There are two major difficulties when trying to detect crest lines in gray-tone images. First, crest lines are generally not iso-level lines: the luminance varies, the lines are dotted; a prior reconnection of the lines sections is required before engaging their extraction. Second, when images are noisy or fuzzy, crest lines are often irregular and a geometrical regularization is necessary.

The problem of regularizing thin crest lines in gray-tone images has been addressed in previous works [4–6, 8] and has led to the powerful concept of viscous transformation.

What is the fundamental idea of the viscous transformations ? Basically, morphological filtering is based on openings or closings. The shapes in images are simplified according to a structuring element having a predefined

G. Banon, et al. (eds),
Mathematical Morphology and its Applications to Signal and Image Processing, 189–200.

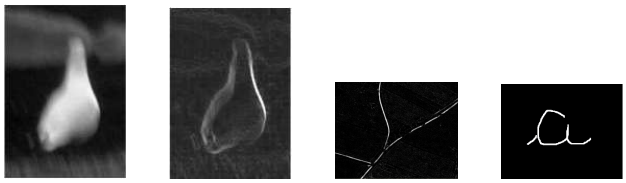

(a) (b) (c) (d)

Figure 1. Some applications where crest lines have to be detected on gray-tone images. (a) Original gray-scale image. (b) its gradient. Crest lines of the gradient image correspond to the shapes edges. (c) A problem of road detection in a gray-tone air image. (d) A hand writing example (in a binary image).

shape and size. The filtering activity increases with the size of the structuring element. In classical gray-tone morphology, the same transformation is applied on all level sets of the function.

For different reasons, it is often necessary to adapt the regularization to the local luminance information available in the images: structures of high luminance are supposed to be perfectly known while structures of low luminance require a higher amount of modeling. The idea of the viscous transformations is to combine the effects of a whole family of closings (or openings) of decreasing activity in such a way that low luminance areas are severely smoothed whereas points of high luminance are left unchanged.

Two different combinations where proposed in [8] inspired by the behavior of viscous fluids. The first mimics the propagation by an oil type fluid, the second by a mercury type fluid. It has been proven in [8] that the two models are equivalent for functions which are cylinders, i.e., functions made of thin crest lines (of one pixel thick) and of null points.

In [5] viscous closings have been extended to any family of increasing operators of decreasing activity, as for example families of dilations. The present paper will show how dotted thin crest lines in gray-tone images may be reconnected and at the same time smoothed using viscous transformations. As we will see, this idea is not completely new.

The questions we mentioned are completely classical in the binary case. However, their resolution in the case of numerical functions raises some difficulties. A binary example is presented in Figure 2. By closing, irregular portions of the curve are enlarged while linear ones are left unchanged. A smoothed and thin version of the original curve is very easily obtained by extracting the median axis of the closed set. In this example, the median axis is computed by successive morphological thinning. Of course, the structuring element used must be homotopic [1, 7].

Independently of the smoothing, the question of the connection of the different curve portions is very easily solved by the use of the distance function.

(a) (b) (c)

Figure 2. Regularization of a thin line by closing. (a) Original binary image. (b) Result of a closing by a disk. (c) Extraction of the median axis by homotopic thinning.

(a) (b) (c) (d) (e)

Figure 3. (a) Original binary image. (b) Distance map computed on a narrow band. (c) Homotopic numerical thinning of the distance map. (d) Crest lines of the thinned image. (e) Crest lines remaining after pruning.

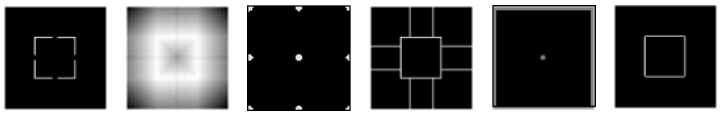

(a) (b) (c) (d) (e) (f)

Figure 4. Standard morphological algorithm for connecting binary contours. (a) Dotted square. (b) Inverse distance function. (c) Inverse distance function and its regional minima (corresponding to the the ultimate eroded of the negative original set). (d) Watershed line of the inverse distance function. (e) Original square and imposed markers. (f) Watershed line associated to a set of markers.

Let X represents a thin binary structure made of several connected components and suppose that we want to join the components of X in order to produce a unique thin connected set while minimizing the length of the final structure. The standard method in the binary case consists in two steps:

- first, the computation of the distance of any point x of the space to the set X. This step issue is the formation of a distance map f_d:

$$f_d(x) = d(x, X) = \inf\{d(x, y),\ y \in X\}. \tag{1.1}$$

  Of course, $f_d(x) = 0$ if x belongs to X. Note that the connected components of X are the regional minima of f_d.

- second, the extraction of the minimal paths in f_d connecting the set X. Or equivalently, detecting the saddle points and their downstream, yielding the so-called perceptual graph [3], which can also be done

$$\begin{array}{ccc} f & \longrightarrow & \{\chi_h(f)\}_{h\geq 0} \\ & \text{decomposition} & \\ \| & & \downarrow \mathrm{Id} \\ \bigvee_{h\geq 0} h.\chi_h(f) & \longleftarrow & \{\chi_h(f)\}_{h\geq 0} \\ & \text{reconstruction} & \end{array}$$

Figure 5. Level set decomposition and reconstruction of an upper semi-continuous function

$$\begin{array}{ccc} f & \longrightarrow & \{\chi_h(f)\}_{h\geq 0} \\ & \text{decomposition} & \\ T_N^v \uparrow & & \downarrow T_{N-h} \\ \bigvee_{h\geq 0} h.T_{N-h}[\chi_h(f)] & \longleftarrow & \{T_{N-h}[\chi_h(f)]\}_{h\geq 0} \\ & \text{reconstruction} & \end{array}$$

Figure 6. The oil model viscous transformation: each level set is processed independently

by extracting the most significant crest lines of the inverted distance function. As a particular case, overlapping particles may be separated by computing the watershed line of the inverted distance function.

This very classical algorithm is illustrated in Figures 3 and 4. In practice, only interesting crest lines are selected. The watershed transform associated with a predefined set of markers is one of the most elegant solution for this task (see Figure 4). In the example presented in Figure 3 however, the standard algorithm has been modified: the distance map is computed in a narrow band (of width 20 pixels); it is then thinned by an homotopic numerical thinning [1,7]. The regional minima being eliminated, the final set results from a morphological pruning of the crest lines.

The purpose of the work presented in this paper is to extend the procedure developed for binary sets to gray-tone images. This will be possible thanks to the viscous dilations. The general framework of viscous transformations being recalled in the next section, viscous dilations are then introduced and their properties studied. Several examples are then presented for illustrating the pertinence of the proposed method.

2. Viscous transforms

Viscous transformations were firstly introduced for regularizing the watershed transform but their applications field largely exceeds the strict segmentation framework. What we discuss here was essentially already developed in [8]. The current presentation is however notably different. In [8], only viscous closings were studied; in the present paper, the concept is enlarged to any increasing operator as suggested in [5].

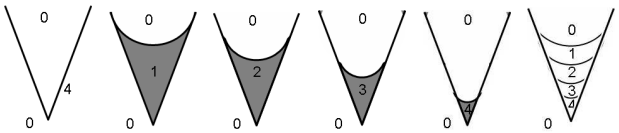

(a) (b) (c) (d) (e) (f)

Figure 7. Viscous transformation (oil type). T_n correspond to closings; (a) f is a thin angular line. (b)$1.T_{N-1}[\chi_1(f)]$ (c) $2.T_{N-2}[\chi_2(f)]$ (d) $3.T_{N-3}[\chi_3(f)]$ (e) $4.T_{N-4}[\chi_4(f)]$ (f) $T(f) = \bigvee_{h\geq 0} h.T_{N-h}[\chi_h(f)]$.

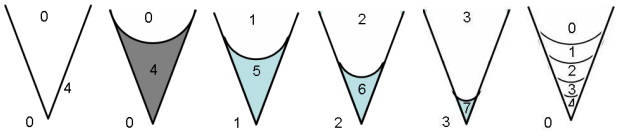

(a) (b) (c) (d) (e) (f)

Figure 8. Viscous transformation (mercury type). (a) f (b) $T_N[f]$ (c) $T_{N-1}[f+1]$ (d) $T_{N-2}[f+2]$ (e) $T_{N-3}[f+3]$ (f) $T(f) = \bigwedge_{h\geq 0} T_{N-h}[f+h]$.

Let us consider a family of morphological operators of increasing activity. By morphological, we mean increasing operators. Let $(T_n)_{n=0:N-1}$ denotes the family. T_n being increasing, it preserves the order between sets or functions: $f < g \Rightarrow T_n(f) < T_n(g)$.

T_n being of increasing activity means: if $n > p$, $T_p(f)$ is closer to f than $T_n(f)$. If, in addition, the T_n are supposed to be extensive, this leads to: $Id = T_0 < T_p < T_n$

Well known examples of such families are the granulometries (by opening or by closing) or the pyramid of dilations or erosions (associated with homothetic convex structuring elements). In order to simplify the presentation, we restrict ourselves to extensive operators (closings or dilations for example); the case of anti-extensive operators is dual; the case of auto-dual operators is more delicate and will not be treated here.

Rather than computing each filter resultant one by one as is the case in granulometric analysis, the idea of the viscous transformations is to combine the effects of the whole family of filters in a unique formulation. The image points are not anymore identically processed. The filtering parameter n is adapted to the local luminance so that regions with low luminance are strongly smoothed whereas regions of high luminance are left unchanged.

The first solution consists in examining the function level set by level set and in indexing the filtering parameter n to the level h: $n = N - h$ for example.

Let $X_h(f)$ and $\chi_h(f)$ denote the level set of the function f at level h

and the associated indicatrix function:

$$X_h(f) = \{x \in E,\ f(x) \geq h\} \quad \text{and} \quad \chi_h(f) = \begin{cases} 1 & \text{if } x \in X_h(f) \\ 0 & \text{otherwise.} \end{cases} \tag{2.2}$$

The function f is supposed to be positive so $h \geq 0$, and of course upper semi-continuous so $\forall h \geq 0$, $X_{h+1}(f) \subset X_h(f)$, and

$$f = \bigvee_{h \geq 0} h.\chi_h(f), \tag{2.3}$$

which means that f can be processed level set by level set if the process is increasing (see Figure 5). As example, T_n being supposed to be increasing, it satisfies:

$$T_n(f) = \bigvee_{h \geq 0} h.T_n[\chi_h(f)]. \tag{2.4}$$

If now n depends of h ($n = N - h$), the level set decomposition leads to the following definition (see Figure 6):

$$T_N^v(f) = \bigvee_{h \geq 0} h.T_{N-h}(\chi_h(f)). \tag{2.5}$$

T_N^v corresponds to the *oil model* described in [8]. For illustration, let us consider a thin line presented in Figure 7. T_n being extensive, the thin line is enlarged by T_n; the cone's interior is smoothed by decreasing size openings: it grows as a viscous lake does, if one interprets the altitude h as a temperature and the filtering parameter $(N - h)$ as a viscosity indicator.

Rather than indexing the filtering parameter n on the luminance h, it can be more interesting to index it on the contrast. The reasoning leading to the second viscous transformation model is detailed in [8]. It is inspired from the behaviour of a *mercury type of fluid*:

$$\tilde{T}_N^v(f) = \bigwedge_{h \geq 0} T_{N-h}(f + h).$$

The mercury type viscous transformation behavior is illustrated on Figures 8 and 9. In both oil and mercury cases, the results of filters T_n when n varies, are stacked. It has been proved in [8] that these two models are equivalent in the case where the function is a set of cylinders on top of a background of value 0.

3. Viscous openings and closings

As said previously, operators T_n may be any extensive morphological transformation whose activity decreases with n and notably closings. As example, viscous closings are defined as follow:

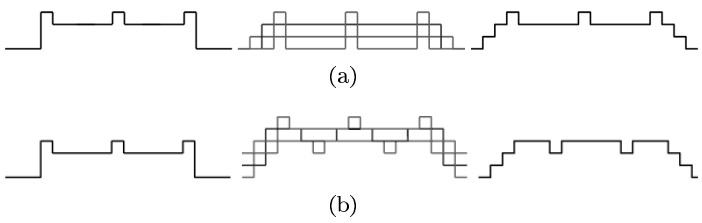

Figure 9. Difference between oil and mercury type of viscous dilation. (a) In the first case (the oil type), details of high luminance are preserved. (b) In the second type (the mercury type), the filtering activity is function of the contrast and not of the luminance.

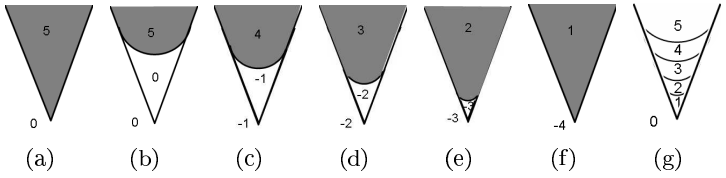

Figure 10. Viscous opening. (a) Original set. (b-f) Results of openings by disk of decreasing size. (g) Result of the viscous opening. Details of the original shape are associated with low levels and coarse descriptions to high levels.

$$\varphi^v_{R_0}(f) = \bigvee_{h\geq 0} h.\varphi_{R_0-h}(\chi_h(f)) \text{ and } \tilde{\varphi}^v_{R_0}(f) = \bigwedge_{k\geq 0} \varphi_{R_0-k}(f+k), \qquad (3.6)$$

where $R_0 - h$ is the size of the structuring element.

The viscous openings expressions are derived by duality. However, the formulation is simpler in the mercury case than in the oil case. In the mercury case, it expresses as follow:

$$\tilde{\Gamma}^v_{R_0}(f) = \bigvee_{k\geq 0} \gamma_{R_0-k}(f-k). \qquad (3.7)$$

Let us now examine what kind of images are build via viscous openings. The Figures 10 and 11 illustrate viscous openings behavior. In these of the set presented in Figure 10, oil and mercury models are equivalent. This example of Figure 11 illustrates the openings granulometric property [2]: details and coarse shapes are represented at opposite granulometric scales. The viscous transform gathers the entire granulometric information in a unique formulation where coarse sets and details are stacked: due to the size-brightness correlation, details of shapes of low luminance are lost; the luminance of the smallest shapes is lowered. Viscous closings have a dual

(a) (b) (c)

Figure 11. Effect of the viscous opening. (a) Original image of bubbles. (b) Result of a standard opening by a Euclidian disk of size 20. (c) Result of a viscous opening of size 20. Here, the mercury model is chosen since the image is made of catchment basins located at different altitudes.

effect on crest lines as illustrated in Figures 12 and 13. After a viscous or non viscous closing, a thin line is very simply restored by thinning.

4. The viscous dilations

We arrive now at the heart of the paper: the relation between distance maps and viscous transforms and their use for reconnecting structures in gray-tone images.

Let us consider a binary set X in a space E. We want to compute the Euclidean distance from any point $x \in E$ to X. When restricting ourselves to the discrete case, the distance map (also called distance function) can easily be computed via erosions by disks of increasing size. And conversely, the negative distance map is computed via dilations of increasing size. Let δ_n denote the dilation by an Euclidean disk of radius n. Any point belonging to the dilated set $\delta_n(X)$ is at a distance lower or equal to n from X:

$$x \in \delta_n(X) \Leftrightarrow d(x, X) \leq n. \tag{4.8}$$

Considering functions rather than sets:

$$\delta_n(\chi)(x) = 1 \Leftrightarrow d(x, X) \leq n, \tag{4.9}$$

where $\forall x \in E$, $\chi(x) = 1$ if $x \in X$ and $\chi(x) = 0$ otherwise. χ is nothing but the numerical function of value 0 or 1 defined on the space E and associated with the binary set X.

The computation of the distance map in a narrow band of size $N - 1$ around X involves the partial sum:

$$\sum_{n=0}^{N-1} \delta_n(\chi) \text{ with } \sum_{n=0}^{N-1} \delta_n(\chi)(x) = \begin{cases} N & \text{if } x \in X, \\ N - n & \text{if } d(x, X) = n, \\ 0 & \text{if } d(x, X) \geq N. \end{cases} \tag{4.10}$$

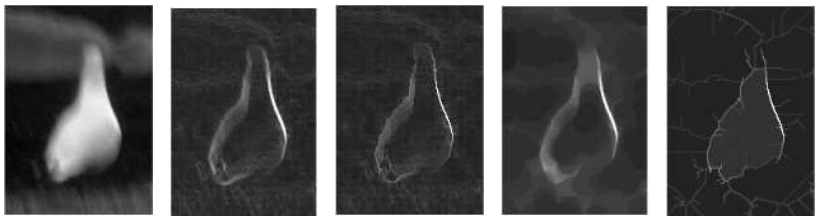

(a) (b) (c) (d) (e)

Figure 12. (a) Original image. (b) Its morphological gradient. (c) The homotopic thinning of the gradient. (d) Standard closing of the gradient. (e) Homotopic thinning of (d)

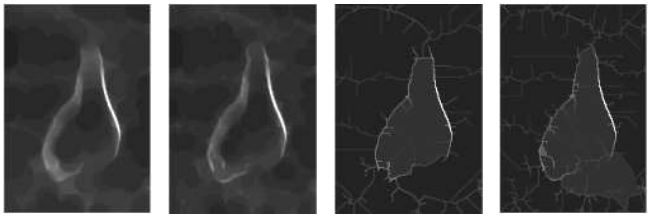

(a) (b) (c) (d)

Figure 13. Effect of the viscous closings on the gradient image. (a) Mercury model. (b) Oil model. (c-d) Homotopic thinning of (a-b). Note that, only the oil model preserves the crest lines of low contrast.

The points of the set X form the crest lines of the negative distance function. Moreover the operator $\sum_{n=0}^{N-1} \delta_n(\chi)$ is nothing but a viscous dilation. Indeed, the sets $\delta_n(X)$ are nested: $X = \delta_0(X) \subset ... \subset \delta_n(X) \subset ... \subset \delta_{N-1}(X)$. Points belonging to $\delta_n(X) \setminus \delta_{n-1}(X)$ are at distance n from X. Instead of summing the dilated sets, the distance function can be computed by translating and superposing the dilated sets:

$$\sum_{n=0}^{N-1} \delta_n(\chi) = \bigvee_{n=1}^{N} n.\delta_{N-n}(\chi) = \bigvee_{n=0}^{N} n.\delta_{N-n}(\chi), \tag{4.11}$$

where $n.\chi$ corresponds to the set X represented with the luminance n.

Suppose now that the set X is replaced by a cylinder of high N and let f denote this function. All level sets $X_h(f)$ are identical if $0 \leq h \leq N$ and empty for $h > N$. This example allows to rewrite the precedent formulation for functions as follow:

$$\bigvee_{h \geq 0} h.\delta_{N-h}(\chi_h(f)). \tag{4.12}$$

Figure 14. Principle of the viscous dilation (oil type of fluid). The original function level sets are dilated then stacked. The viscous dilation results from a supremum.

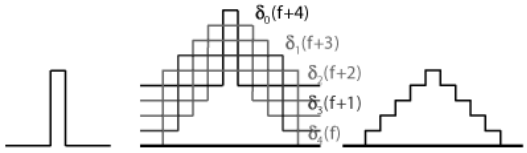

Figure 15. Viscous dilation computation (case of a mercury type of fluid). The original function is shifted then dilated. The original dilation results from an infimum.

Figure 16. Effect of the viscous dilations on walls of different altitudes (case of a oil type of fluid).

This expression as to be compared to the oil type viscous transformations:

$$T_N^v(f) = \bigvee_{h\geq 0} h.T_{N-h}(\chi_h(f)). \tag{4.13}$$

The similitude is illustrated in Figure 14: dilations of decreasing activity are progressively stacked as it was the case for the oil model viscous transformations. As a consequence, distance functions may be interpreted as viscous transformations associated with dilations of decreasing activity. We will call this transformation *viscous dilation*.

By analogy with viscous closings two viscous dilations (inspired from the oil and the mercury models) may be defined:

$$\delta^v(f) = \bigvee_{h\geq 0} h.\delta_{N-h}(\chi_h(f)) \quad \text{and} \quad \widetilde{\delta^v}(f) = \bigwedge_{h\geq 0} \delta_{N-h}(f+h). \tag{4.14}$$

These transformations are illustrated on Figures 14, 15 and 16.

Of course, these transforms are equivalent to the sum $\sum_{n=0}^{N-1} \delta_n(f)$ for binary functions but the three transformations differ in the case of gray-scale functions.

As an illustration, the viscous transformations have been tested on gray-scale images: in the Figures 17, the goal is the segmentation of the bird.

(a) (b) (c) (d) (e)

Figure 17. (a) Original image. (b) Gradient image. (c) Associated watershed transform. (d) Viscous dilation of the gradient image. (e)Associated viscous watershed transform (watershed computed after viscous closing of the relief).

The bird is first roughly localized. Then, the gradient norm of the original function is computed. For reference, we present the segmentation obtained by computing the watershed transform directly on the original gradient image. A more robust segmentation can be obtained if a viscous dilation is applied on the gradient before computing the watershed transform. And a more regularized solution is obtained if, in addition to the viscous dilation, the standard watershed is replaced by the viscous watershed. We recall that the viscous watershed is a standard watershed computed after a viscous closing of the relief.

Another example is presented on Figure 18. The original image is first thinned, then a viscous dilation is computed and the derived image is thinned. So, one can observe how crest lines are connected. The result obtained via oil and mercury types of viscosity are compared. Lastly, watersheds are computed and compared.

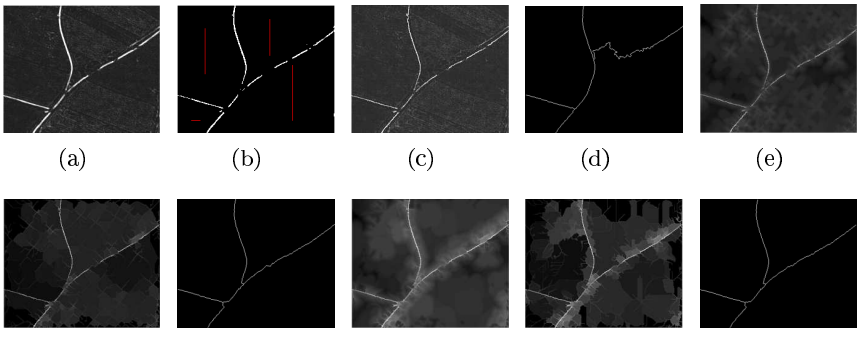

(a) (b) (c) (d) (e)

(f) (g) (h) (i) (j)

Figure 18. (a) Original image. (b) Markers. (c) Thinned original image. (d) Watershed segmentation. (e) Viscous dilation of the thinned original image (oil model). (f) Thinning of the result of the viscous dilation. (g) Watershed segmentation. (h-j) The same than (e-g) using the mercury model.

The viscous dilation allows to reconnect disconnected contours portions while viscous closings have a regularization effect. It is possible to combine the advantage of both dilations and closings by considering the family of the closing dilated sets. For the "oi" model, it expresses as:

$$\bigvee_{h\geq 0} \varphi_{r(h)}\delta_{r(h)}(h.\chi_h(f)).$$

5. Conclusion

Viscous transformations appear to be extensions to grey-tone functions of distance functions or opening function of binary sets (sum of dilations or openings of increasing size). As distance functions of binary sets are useful for connecting binary dots or separating particles, viscous dilations are useful for filling missing gaps in grey-tone contours. They may be used besides or in conjunction with viscous closings in order not only to fill in gaps but also to regularize the contours of gray-tone images. In a next paper we will further study the properties of these transformations.

References

[1] S. Beucher, *Segmentation d'images et morphologie mathématique*, Ecole des Mines de Paris, Fontainebleau, France, 1990.

[2] G. Matheron, *Eléments pour une Théorie des Milieux Poreux*, Masson, Paris, 1967.

[3] F. Meyer, *Skeletons and Perceptual Graphs*, Signal Processing **16** (1989), no. 4, 690–710.

[4] F. Meyer and C. Vachier, *Image Segmentation based on Viscous Flooding Simulation*, Mathematical Morphology and its Applications to Image and Signal Processing (2002), 69–77.

[5] ———, *On the Regularization of The Watershed Transform* (P. W. Hawkes, ed.), Academic Press, 2007, Advances in imaging and electron physics, pp. 195–251.

[6] J. Serra, *Viscous Lattices*, Journal of Mathematical Imaging and Vision **22** (2005), 269–282.

[7] P. Soille, *Morphological Image Analysis (Principles and Applications)*, Springer-Verlag, 1999.

[8] C. Vachier and F. Meyer, *The Viscous Watershed Transform*, Journal of Mathematical Imaging and Vision **22** (2005), 251–267.